Sections and Chapters

Gubert Farnsworth

Contents

1 Introduction

2 Background

2.1 Convolutional Neural Networks

Convolutional Neural Networks, also known as ConvNets or CNNs, are the state-of-the-art neural networks for most computer vision tasks, such as image classification and object detection or face recognition.

Unlike regular feed-forward neural networks based on fully-connected layers of neurons, ConvNets are trained to learn relatively small filter kernels, that can extract valuable information from different areas of an image. Therefore, they reduce the amount of training parameters significantly and are able to train also on large images.

2.1.1 Convolution

The cornerstone of ConvNets are the convolutions, represented in Figure 1. Convolutions are based on small filters, which run through the image and sum the multiplications of each input value with the corresponding filter value. Each filter must have the same amount of channels as the input, the width and height are optional.

2.1.2 Convolutional Layers

In the first layers of a network, each filter usually extracts some low-level feature, such as horizontal or vertical edges. The output of the convolution, are the outputs of each filter stacked in the channel dimension. As the convolutions get deeper into the network, they start to combine these low-level features, to higher level features, such as an eye or a mouth.

2.2 Generative Adversarial Networks

Introduced in 2014 [13], generative adversarial networks, so-called GANs, have been the focus of countless research papers and creative implementations. GANs have learned how to generate an image of a cat from a simple drawing [14],

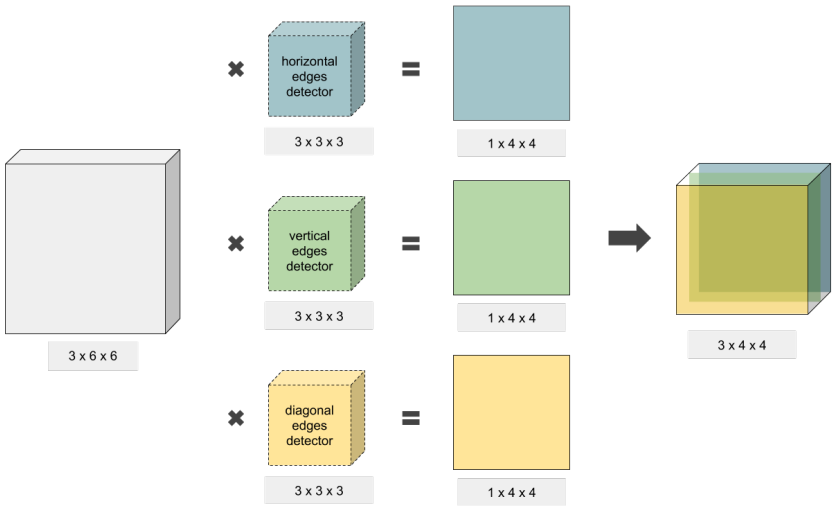

Figure 1: **Convolution.** The input image is convolved with 3 filters, each one detecting a different low-level feature. The final output is the output of each convolution stack in the channel dimension.

create new artworks [30], generate high-resolution celebrity faces [19], colorize grayscale images and much more.

In order to generate new samples, two neural networks are trained to compete against each other. A common analogy can be found in coin forgery: while a fraud investigator is trying to detect real coins from fraudulent ones, the coin forger is trying to improve the falsification, so that the investigator is unable to tell the difference.

In computational world, the investigator is a neural network called *Discriminator* competing with the forger network called *Generator*. The discriminator is trained to classify samples from the original dataset as "real", and samples generated by the generator as "fake". The generator is trained to fool the discriminator, so that it cannot correctly classify the generated samples as fake.

Figure 2 shows example data points of the hand-written digits dataset MNIST [23], along with samples generated with a deep convolutional GAN [20] - the samples from the original and generated distributions are almost indistinguishable.

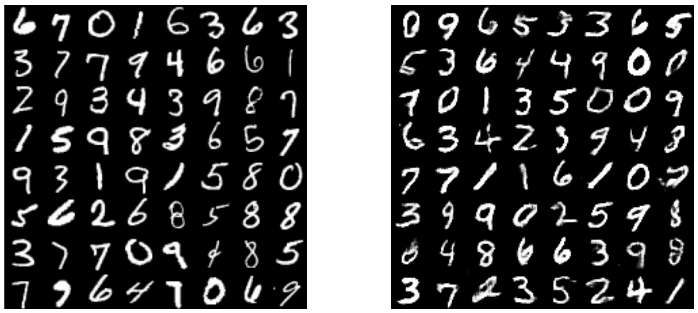

(a) Original MNIST (b) Generated MNIST

Figure 2: **MNIST Example.** (a) Example of data points in the original MNIST dataset [23]. (b) Samples generated with a Deep Convolutional GAN [20].

2.2.1 Architecture

Figure 3 describes a typical GAN architecture. The discriminator is a common Convolutional Neural Network [22], which takes an image as input and is trained to find filters that extract necessary information in order to classify the image. The output is a 1-dimensional vector - or in case of GANs, a scalar value, classifying the image as real or fake.

The generator's architecture is similar, however it uses a transposed convolution, the so-called "deconvolution", to produce a 2 or 3-dimensional output from a 1-dimensional input vector. The generator input vector is sampled randomly.

The classification output of the discriminator is back-propagated through the discriminator, as well as the generator network, in order to adjust the networks' weights to improve the training objective.

2.2.2 Training Objective

Given input data with distribution $p(x)$, the generator G is a neural network, that maps random input noise z to the input space, as $G(z, \theta_g)$, learning the model distribution $\hat{p}(x)$. The discriminator D is a second neural network $D(x, \theta_d)$ with a single scalar output, classifying the input as real, sampled from $p(x)$, or as fake, sampled from the model distribution $\hat{p}(x)$.

The training objective of the discriminator is to maximize the probability of assigning the correct label, while the objective of the generator is to minimize this probability. The loss function of the GAN can be described as the minimax objective,

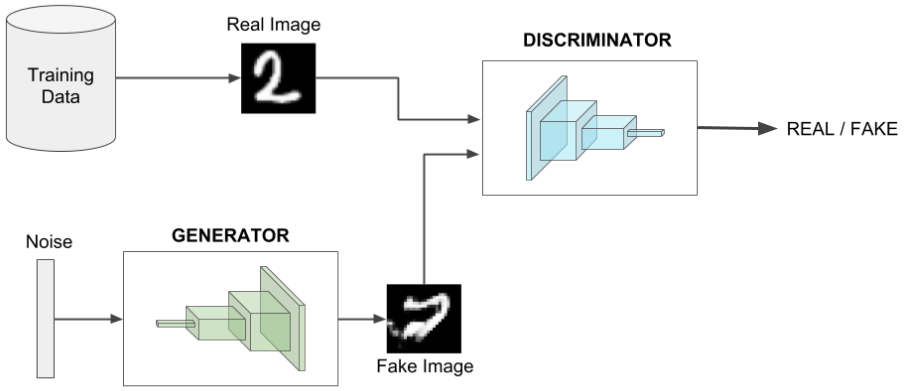

Figure 3: **GAN model.** The generator network produces fake images, which the discriminator network tries to distinguish from the real samples coming from the dataset.

$$\min_G \max_D V(D,G) = \mathbb{E}_{x\sim p_{data}(x)}[\log D(x)] + \mathbb{E}_{z\sim p_z(z)}[\log 1 - D(G(z))]. \quad (1)$$

In order to prevent vanish gradients, as a result of the discriminator saturating by confidently classifying the samples before the generator's update, [13] suggests G to be trained to maximize $\mathbb{E}_{z\sim p_z(z)}[\log D(G(z))]$ instead.

The parameters of the discriminator and generator, θ_d and θ_g, are updated using gradient descent algorithms, by back-propagating the gradients of the loss function in respect to each of the networks' parameters.

2.2.3 Training Difficulties

In theory, the minimax game described in equation 1 is played until generator has perfectly modeled the distribution $p(x)$, so that discriminator classifies the authenticity of the samples at random.

In reality, finding the right balance between the two networks can be difficult. If discriminator gets too good at determining which samples are fake, then generator has no chance to learn the distribution. On the other hand, if generator is updated too much, it can collapse too many values of z to the same value of x to have enough diversity to model the distribution.

Because a modification of the weights of the discriminator that decrease

2.2.4 Deep Convolutional GANs

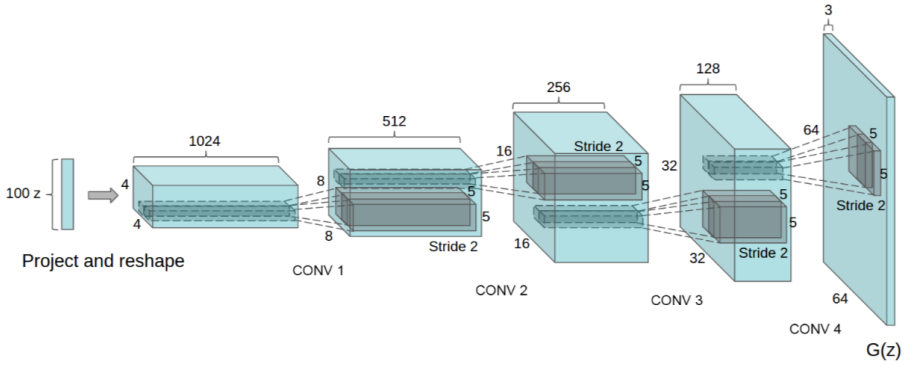

Figure 4: **DCGAN Generator.** An example architecture of a DCGAN generator $G(z)$. The random input noise z is mapped to a 64x64 image with 3 color channels via fractionally-strided convolution layers. Figure reprinted from [28].

Many GAN implementations base their network architecture on Deep Convolutional GANs, described by [28]. The authors introduced architectural guidelines for convolutional networks used in GANs, that stabilize the training and result in more realistic outputs.

After experimenting with CNN architectures commonly used in computer vision tasks, Radford et al. have found that this set of architecture modifications has a positive effect on the stability and convergence speed of the models:

- **All Convolutional Net**: A common practice in convolutional neural networks are *Pooling Layers*, which reduce the number of parameters by filtering the convolution outputs, taking maximum or average of a given region. However, the authors have found that using an All Convolutional Network [32], which replaces all pooling layers with a strided convolution, leads to more stable results.
- **Fully-Connected Layers**: The authors argue, that avoiding fully-connected layers deeper in the network stabilizes the network. Removing all fully-connected layers stabilizes the network, however it slows down the convergence. Therefore fully-connected layers are kept in the discriminator output layer and generator input layer.
- **Batch Normalization**: Batch Normalization [17] has been introduced in common image-classification to make models more robust to parameter initialization and speed up training. The DCGAN paper shows that including a batch-norm layer in all GAN layers (except discriminator output

and generator input), helps generators start learning and produce diverse outputs.

- **Activation Functions**: As opposed to maxout activation suggested by the original GAN paper [13], GANs seem to benefit from *Leaky ReLU* activation function in discriminator, and *ReLU* activation function for generator, except last *tanh* layer.

2.2.5 Conditional GANs

In order to influence the output of a GAN, [25] introduced the Conditional Generative Adversarial Networks. By conditioning both the discriminator and the generator on additional information, the generator learns to output realistic samples given a condition.

Considering the previous example of MNIST hand-written digits synthesis, one can condition the networks using the digits as class labels, and control the network to generate an image of a specific digit. There have also been experiments with text-to-image translation [29], where the network is conditioned on a text description of an image, and various image-to-image translations such as [33], [33], [27].

The training objective of conditional GAN is following:

$$\min_G \max_D V(D,G) = \mathbb{E}_{x\sim p_{data}(x)}[\log D(x|c)] + \mathbb{E}_{z\sim p_z(z)}[\log 1 - D(G(z|c))]. \quad (2)$$

The conditioning information c, such as a class label, text, or another image, is fed to both discriminator D and generator G as additional input layers.

3 Analysis

3.1 Data

As in most machine learning algorithms applied to visual tasks, the quantity and quality of training data is essential to produce high-quality results. It is also common, that data collection and data cleaning make up a significant part of a machine learning project.

In case of fashion images, there are several open-source datasets published online. However, after careful evaluation I have not found them sufficient for the purpose of this thesis. Therefore I have created an application to scrape online fashion stores and download images of fashion products and their description in a computer-readable format.

3.1.1 Requirements

In order to generate high-quality outputs using GANs, the collected dataset should fulfill the following requirements:

1. The fashion products should be photographed on a white background.
2. There should be a machine-readable description of each product, such as color, shape, category, etc.
3. The images should be in a sufficient resolution.
4. There should be a sufficient amount of images of various items.

I have defined these requirements on based on my previous experience with generative algorithms. It is generally easier for the algorithm to focus on the important attributes of the images, if there are no distractions in terms of different model poses, backgrounds, etc. And since the main point of the project is to modify different attributes of the products, the images need to be labeled.

3.1.2 Existing Fashion Datasets

I have evaluated several existing fashion datasets, however none of them satisfied the criteria for this thesis.

DeepFashion

The Deep Fashion Set [24] includes more than 200.000 images of clothing images, labeled with 1000 attributes. However, this dataset does not fulfill the first requirement - its clothing items are photographed on people in various poses and backgrounds. This type of variation might be too complex for the algorithms and can lead to unsatisfactory results.

Fotolia

Another available option, that has been provided by Prof. Dr. Barthel, is the Fotolia image dataset, which can be explored on the picsbuffet website [5]. To test the dataset, I have chosen all images with keywords "dress" and "isolated" and compared them to a template image, based on the distance between their 64-dimensional feature vectors calculated via Akiwi API [31]. Figure 5 shows the results of this search. Additionally to an undesired low resolution of the returned images - around 100 x 160 pixels - the results also have too much variety, such as different model poses, different zoom levels and backgrounds. The description of the images did not include many useful attributes, with most pictures being labeled with words such as: "beauty", "young", "person", and lacking information about colors, shapes and pattern.

(a) Template Image (b) Fotolia Images

Figure 5: Fotolia images with keywords "dress" and "isolated" with closest feature vector distance from the template image.

3.1.3 Scraped Dataset

Based on the evaluation of existing fashion datasets, I have identified a need for creating a new dataset specifically for the requirements of the application. I evaluated several fashion e-shops, from which images of the products and their descriptions could be downloaded.

I chose 3 websites, based on the structure and amount of information they provide: zalando.de, aboutyou.de and fashionid.de. Each of them provides several thousand fashion products for women and men, with a photograph of the item on a white background and some basic description such as color, pattern, shape, length etc. For simplicity, I have limited the dataset to women's clothes, excluding products like accessories and shoes.

The *Fashion Scraper* is a python project, that scrapes images and data from all the mentioned websites and saves them locally for further processing, such as image processing, data cleaning, and description translating. This project was part of my Independent Coursework and the documentation of the project can be found in Attachments, or on github.com/sonynka/fashion_scraper.

Figure 6: **Examples of images in the final dataset.** Each column contains images from different category as follows: blouses, dresses, jackets, knitwear, pants, skirts, tops.

The scraped dataset consists of 92.200 images of size 256x256 pixels in JPEG format. The images are split into folders by categories and the whole dataset is described in a CSV file, which includes the following information:

- **id**: ID of the product as defined by the website (SKU)
- **img_path**: relative local file path to the saved product image
- **img_url**: URL to the product image file hosted on the seller website
- **model_img_urls**: URLs to the images of the product worn by models
- **product_url**: if given, the URL to the product listing on the website
- **brand**: product brand as displayed on the website
- **name**: product name as displayed on the website
- **attributes**: list of product attributes listed on the website in German, such as shape, length, material, size etc.

In addition to the website data, there are columns that contain processed and translated data. Below is the list of the column names and the values they can take.

- **category**: blouses, dresses, jackets, knitwear, pants, skirts, tops
- **color**: beige, black, blue, gray, green, pink, red, white, yellow
- **length**: 3-4, knee, long, normal, short or no value
- **sleeve_length**: half, long, short, sleeveless or no value
- **fit**: loose, normal, tight or no value
- **pattern**: floral, lace, polkadots, print, stripes, unicolors or no value
- **neckline**: back, deep, lines, round, v, wide or no value

There is also a CSV file that contains a list of image file paths and binary classification of the list of values mentioned in the above list.

A table with all attributes and num of images will be in attachments

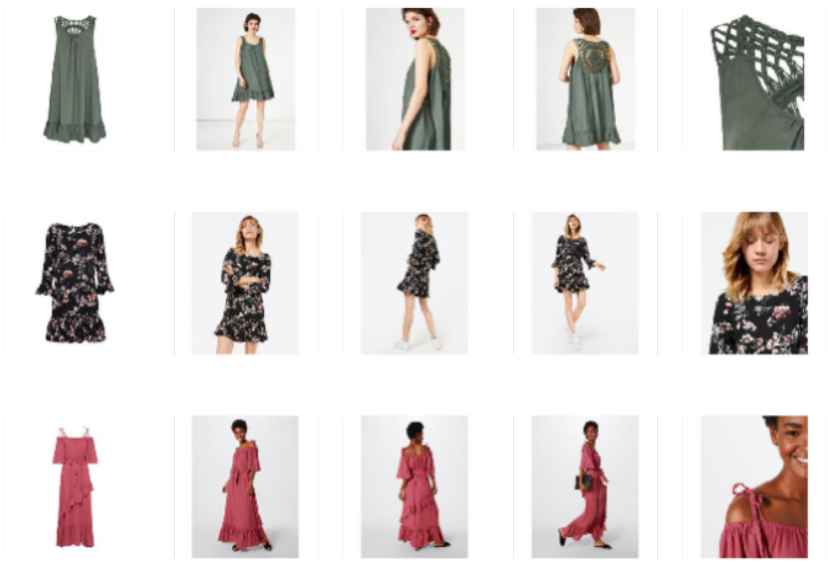

Figure 7: **Examples of model images in the dataset.** First column shows the product images and the other columns show images of models wearing the given product in various poses and level of detail.

Model Images

For some tasks of this work, I have also downloaded an extra dataset of images of products worn by models from the scraper websites. The model images are of size 256x256 pixels in JPEG format and the file names correspond to the file names of the product images. Each product has variable amount of corresponding model images, varying in model poses, zoom level and detail level of the photo (see Figure 7).

Characteristics	pix2pix	CycleGAN	StarGAN	MUNIT	FaderNets
Supervised	Yes	No	No	No	No
Multi-Domain	No	No	Yes	No	No
Multi-Modal	No	No	No	Yes	No
Latent Space	No	No	No	Yes	Yes

Table 1: **Comparison of existing GAN models based on their characteristics.**

3.2 Image-To-Image Translation

Image-To-Image Translation using GANs has been widely researched in the past few years, with creative approaches and models published regularly. For the purpose of this thesis, I have reviewed and tested some of these projects, to evaluate what results can be achieved on the fashion dataset and which GAN is best suited for what task.

Table 1 shows the comparison of 5 evaluated networks: *pix2pix* [18], *CycleGAN* [34], *StarGAN* [12], *MUNIT* [16] and *FaderNetworks* [21], for which I compared the following attributes:

- **Supervised**: Does the network need a dataset consisting of paired images, such as the same skirt in a short and long version.
- **Multi-Domain**: Is the network able to train one model for different domains translations, or does each domain pair require its own trained generator.
- **Multi-Modal**: Is the network able to generate different outputs from the same input.
- **Latent representations**: Does the network train in pixel-space or uses latent representations, such as separate content and style representations.

The following sections describe the characteristics of the evaluated networks, their applications, training process and architecture.

3.2.1 Pix2Pix

The so-called Pi2Pix networks were first introduced by Isola et al. [18] as a framework for image-to-image translations. Some of the applications of Pix2Pix include mapping day photographs to night, sketches of shoes to realistic shoe images or colorizing black-and-white photos.

Pix2Pix uses the concept of conditional GANs [25] (described in Section 2.2.5) to influence the network's output by providing a condition. In case of Pix2Pix, the condition is an image that is to be translated to another domain. To translate images from an input domain to a target domain, the model requires a dataset of paired images (x_{input}, x_{target}), such as a grayscale image and a corresponding color image.

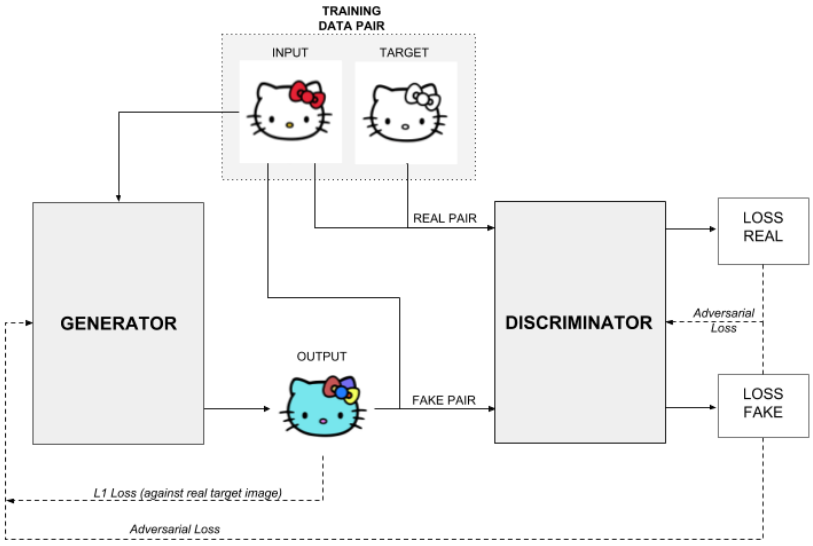

Figure 8: **Pix2Pix Training Process.** Dataset consists of paired input and target images. Generator takes input image as condition to output a generated image. Discriminator tries to predict, given an input image, if the target image comes from dataset or from generator. This output is then used to further optimize both networks. Figure adapted from [15].

As shown in Figure 8, the generator takes the input image x_{input} and tries to map it to the target domain $\hat{x}_{target}$, such as: $G : (x_{input}, z) \rightarrow \hat{x}_{target}$. The discriminator, also conditioned on the input image x_{input}, tries to predict if the target image comes from the data distribution or if it was generated. The discriminator tries to improve these classifications, while the generator tries to prevent correct classification.

Training Objective

The adversarial objective, which G is trained to minimize and D is trained to maximize, can be expressed as following:

$$\mathcal{L}_{adv}(D,G) = \mathbb{E}_{x_{in},x_{trg}}[\log D(x_{in},x_{trg})] + \mathbb{E}_{x_{in},z}[\log 1 - D(x_{in},G(x_{in},z))] \quad (3)$$

Based on the results of previous conditional GAN approaches [27], Isola et. al [18] have also shown, that enforcing the generated output to be closer to the ground truth target by adding a second objective reduces artifacts in the results. They therefore suggest to use the L1 distance as reconstruction loss function for the generator to optimize.

$$\mathcal{L}_{rec}(G) = \mathbb{E}_{x_{in},x_{trg},z}[||x_{trg} - G(x_{in},z)||_1] \quad (4)$$

The final objective of the generator is:

$$G^* = arg \min_G \max_D \mathcal{L}_{adv}(D,G) + \lambda \mathcal{L}_{rec}(G) \quad (5)$$

where λ controls the relative importance of the two loss functions.

Generator

In image translation tasks, it is usual, and even desirable, that the input and target image domains share a common underlying structure. Modeling the generator with a simple encoder-decoder architecture, where all data must pass through a so-called "bottleneck" layer, can therefore result in an undesirable loss of the low-level details that the two domains share.

The authors therefore suggest to base the generator on a U-Net architecture. U-Net contains so-called skip connections, which pass the output directly from the encoder to the decoder, therefore skipping the bottleneck. The generator is therefore able to include low-level features from the input in the output.

Discriminator

The authors of Pix2Pix [18] argue, that while the use of L1 or L2 loss for image generation usually produces blurry outputs, they are sufficient to capture low-level frequencies, for example the colorfulness of the image. Therefore, when combining adversarial loss with an L1 loss, the discriminator only needs to focus on high-level frequencies.

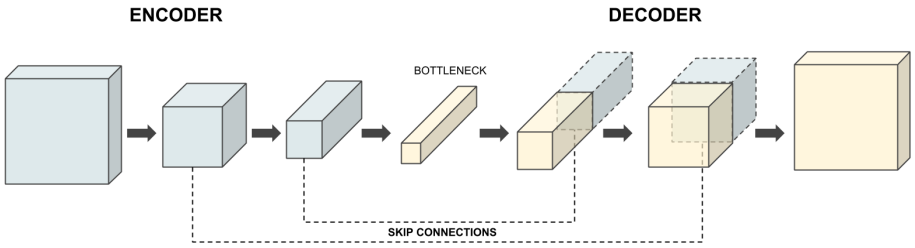

Figure 9: **U-Net Generator.** Skip connections are added between each encoder layer i and decoder layer $n - i$, where n is the total number of layers, so that information can bypass the bottleneck.

They introduce the *PatchGAN* architecture - a discriminator, which evaluates the high-frequency structure of the input image in patches. The PatchGAN discriminator can be described as a convolution running over the input image, classifying each patch as real or fake. The overall classification of an image is then calculated as the average of the decision for each patch. This allows the discriminator to scale efficiently to larger images and, as the authors have shown, forces sharp and colorful outputs.

3.2.2 CycleGAN

CycleGANs [34], unlike Pix2Pix, do not require a paired image set for the image domains to be translated. The unsupervised setting is preferred in most translation tasks, as obtaining image pairs of two domains can be difficult or even impossible - for example translating female faces to male, or Monet artworks to realistic photographs. The assumption hereby is that both image domains share certain underlying visual similarities.

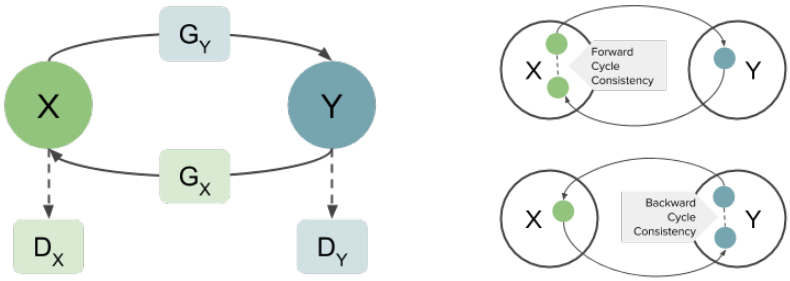

(a) CycleGAN Model (b) Cycle Consistency Loss

Figure 10: **CycleGAN** (a) Themodel consists of two mappings, G_X and G_Y and corresponding discriminators D_X and D_Y. (b) Cycle Consistency Loss measures the L1 distance between a real sample from one image domain and its encoded-decoded version. Figure adapted from [34].

The model consists of two generators, G_X and G_Y, which learn mapping from image domain X to image domain Y, $G_Y : X \rightarrow Y$, and vice versa, $G_X : Y \rightarrow X$. Each of the image domains has its own discriminator, D_X and D_Y, that check if the given image comes from the real distribution of the domain or is translated from the opposite domain.

The adversarial loss is therefore applied to both pairs of networks, (D_X, G_X) and (D_Y, G_Y).

$$\mathcal{L}_{adv}(D_X, G_X) = \mathbb{E}_x[\log D_X(x)] + \mathbb{E}_y[\log 1 - D_X(G_X(y))] \tag{6}$$

Additionally to the adversarial loss, CycleGAN also implements a so-called *Cycle Consistency Loss*, which enforces that an image encoded from one domain to another, can also be reconstructed back to the original domain. The authors argue, that reducing the amount of possible mapping functions can help avoid the network to learn mappings that contradict each other [34].

The *forward cycle consistency* defines that an image x from domain X and its encoded-decoded version should be approximately the same: $G_X(G_Y(x)) \approx x$.

The *backward cycle consistency* defines the same for an image from domain Y.

$$\mathcal{L}_{cyc}(G_X, G_Y) = \mathbb{E}_x[||G_X(G_Y(x)) - x||_1] + \mathbb{E}_y[||G_Y(G_X(y)) - y||_1] \quad (7)$$

Both generators train to minimize and both discriminators train to maximize the final objective, which regulates the relative weight of the adversarial loss against the cycle consistency loss with the hyperparameter λ.

$$\begin{aligned} G_X^*, G_Y^* = arg \min_{G_X, G_Y} \max_{D_X, D_Y} \mathcal{L}_{adv}(D_X, G_Y) \; &+ \mathcal{L}_{adv}(D_Y, G_X) \\ &+ \lambda \mathcal{L}_{cyc}(G_X, G_Y) \end{aligned} \quad (8)$$

Architecture

CycleGAN models are roughly based on Deep Convolutional GANs [28], using the PatchGAN architecture [18] for the discriminator.

3.2.3 StarGAN

One of the disadvantages of Pix2Pix and CycleGAN is the missing possibility of multi-domain translation. If there are more than 2 domains to translate between, one must train a new model for each domain pair. This can be time and computationally intensive.

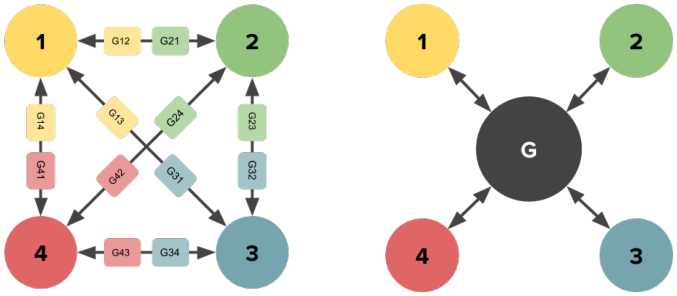

(a) Cross-Domain Models (b) StarGAN Model

Figure 11: **Comparison of cross-domain models and StarGAN model.** While cross-domain models need one generator per each domain pair, StarGAN only trains one generator for multiple domains. Figure adapted from [12].

StarGAN [12] is unique among the tested models, as it is able to train one single generator that maps input to multiple domains, as shown in Figure 14. Using the conditional GAN model [25], the generator is conditioned on a randomly chosen target domain each iteration, so that it can learn mapping for all given domains.

The overall training objective of StarGAN consists of three loss functions:

- *Domain Classification Loss*, which forces the discriminator to also output the domain class of the input image
- *Adversarial Loss*, which is maximized by the discriminator and minimized by the generator
- *Cycle Consistency Loss*, which measures the distance between an original image and its version encoded-decoded by the generator

Domain Classification Loss

Instead of feeding the target domain class c to the discriminator, as in common conditional networks, StarGAN trains the discriminator to classify it. It uses an auxiliary classifier GAN, AC-GAN [26], which forces the discriminator to

output both the probability distribution over the sources of the input, and the probability of the target domain labels, $D : x \rightarrow D_{src}(x), D_{cls}(x)$. This improves the network's stability and performance, as it forces the discriminator to perform and additional task.

This modification to the discriminator introduces the *Domain Classification Loss* with two objectives, L^r_{cls} and L^f_{cls}, optimizing D and G respectively. Given training data with an image x and its original domain c_{in}, D learns to classify the domain label correctly by minimizing the following objective:

$$\mathcal{L}^r_{cls} = \mathbb{E}_{x,c_{in}}[-\log D_{cls}(c_{in}|x)]. \tag{9}$$

The generator objective is to generate images, that fool the auxiliary classifier and are classified as the target domain c_{trg}:

$$\mathcal{L}^f_{cls} = \mathbb{E}_{x,c_{trg}}[-\log D_{cls}(c_{trg}|G(x, c_{trg}))]. \tag{10}$$

Adversarial Loss

Given an image x and a target domain label c_{trg}, generator G tries to minimize the adversarial loss objective, to generate real-looking images conditioned on the target domain, while the discriminator classifying the source of the image, D_{src}, tries to maximize it.

$$\mathcal{L}_{adv} = \mathbb{E}_x[\log D_{src}(x)] + \mathbb{E}_{x,c_{trg}}[\log 1 - D_{src}(G(x, c_{trg}))] \tag{11}$$

Cycle Consistency Loss

Cycle Consistency Loss [34] is used to generate images that preserve the underlying content of the original image, and only change the domain-related attributes:

$$\mathcal{L}_{cyc} = \mathbb{E}_{x,c_{in},c_{trg}}[||x - G(G(x, c_{trg}), c_{in})||_1]. \tag{12}$$

Training Objective

The full training objective for D and G respectively is:

$$\mathcal{L}_D = -\mathcal{L}_{adv} + \lambda_{cls}\mathcal{L}^r_{cls}, \tag{13}$$

$$\mathcal{L}_G = \mathcal{L}_{adv} + \lambda_{cls}\mathcal{L}^f_{cls} + \lambda_{cyc}\mathcal{L}_{cyc}, \tag{14}$$

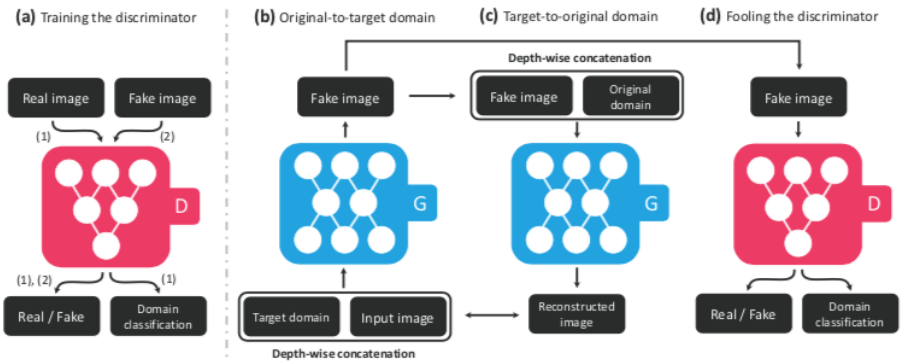

Figure 12: **StarGAN Training Process.** The discriminator classifies the input as real or fake and outputs it's domain class prediction. The generator encodes the image with a target domain, and then decodes the output with the original domain, to calculate the cycle consistency distance. Figure reprinted from [12].

where λ_{cls} and λ_{cyc} control the relative importance of the two loss functions against the adversarial loss.

The model architecture is based on CycleGAN.

3.2.4 MUNIT

All of the introduced models approach the image translation problem as one-to-one mapping. However, many of the image domain translation tasks are in fact multi-modal, meaning one single input can have multiple different outputs. The MUNIT network [16] introduces an unsupervised multi-modal method, which is able to capture the diversity of the output.

Instead of using translation in pixel space, the model tries to model the translation in a latent space. Based on the *partially shared latent space assumption*, a content latent code $c \in \mathcal{C}$ and a style latent code $s_i \in \mathcal{S}_i$ are separated, assuming that the two image domains share a common content space but each has an individual style space.

For each domain, there is an auto-encoder, which consists of a generator G and two encoders: content encoder E^c, and style encoder E^s. Given an image $x \in X$, it is encoded into a content and style code, $E_x^c(x)$ and $E_x^s(x)$. To translate the image $x \in X$ to domain Y, its content code c_x is extracted using the content encoder E_x^c, and it is combined with a random style code s_y, $G_y(c_x, s_y)$.

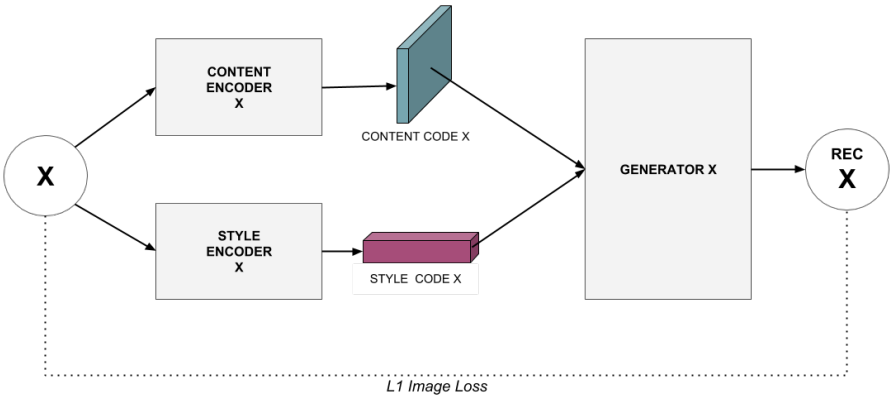

Figure 13: **MUNIT within-domain reconstruction.** An image from domain X is decomposed into content and style code via respective encoders. The decoder is a generator that combines the two latent encodings and translates them back to the original domain. A reconstruction loss is calculated between the original and the reconstructed image to optimize the auto-encoders. Figure adapted from [16].

While the style code is assumed to have a global and simple effect and is therefore sufficiently represented by a low-dimensional vector, the content is assumed to be a high-dimensional vector describing the complex spatial structure of the data.

Reconstruction Loss

The reconstruction loss is similar to the cycle consistency loss [34], enforcing the reconstruction between an image and its latent representation in both directions.

The *image reconstruction loss* encourages the reconstruction of an image after encoding to latent space and decoding back to image space.

$$\mathcal{L}_{rec}^{x} = \mathbb{E}_{x}[||x - G_x(E_x^c(x), E_x^s(x))||_1] \tag{15}$$

The *latent reconstruction loss* consists of a style loss and a content loss, which should be reconstructed after being encoded to image space and decoded back. The content loss enforces the preservation of semantic information of the translated image, while the style loss encourages diversity in the translated outputs.

$$\mathcal{L}_{rec}^{c_x} = \mathbb{E}_{c_x, s_y}[||c_x - E_y^c(G_y(c_x, s_y))||_1] \tag{16}$$

$$\mathcal{L}_{rec}^{s_y} = \mathbb{E}_{c_x, s_y}[||s_y - E_y^s(G_y(c_x, s_y))||_1] \tag{17}$$

The same losses are also applied to image domain Y.

Adversarial Loss

In order to enforce the generated output to look realistic, each domain has a discriminator, D_x and D_y, which is trained to distinguish if the source of the image is the data distribution of the image domain, or if it was generated by the auto-encoder.

$$\mathcal{L}_{adv}^{x} = \mathbb{E}_{c_y, s_x}[log(1 - D_x(G_x(c_y, s_x)))] + \mathbb{E}_{x}[logD_x(x)] \tag{18}$$

The adversarial loss for domain Y is defined similarly.

Training Objective

The overall training objective, which is trained to be maximized by the discriminators and minimized by the generators and auto-encoders can be modified by λ, λ_c, λ_s, controlling the relative weight of each loss:

$$\mathcal{L} = \mathcal{L}_{adv}^{x} + \mathcal{L}_{adv}^{y} + \lambda(\mathcal{L}_{rec}^{x} + \mathcal{L}_{rec}^{y}) + \lambda_c(\mathcal{L}_{rec}^{c_x} + \mathcal{L}_{rec}^{c_y}) + \lambda_s(\mathcal{L}_{rec}^{s_x} + \mathcal{L}_{rec}^{s_y}) \tag{19}$$

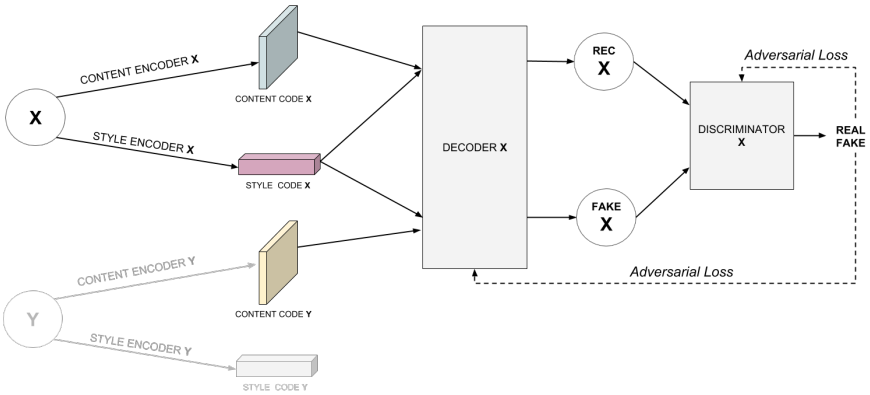

Figure 14: **MUNIT cross-domain reconstruction.** The content code of image from domain Y is combined with style from domain X to generate a fake image X. The discriminator decides if the image was translated or comes from the original image domain based on which the adversarial objective is calculated. Figure adapted from [16].

4 Experiments

The objective of the experiments is to improve image retrieval of fashion products, by allowing the user to perform a series of modifications on the given product image. I have performed most of the experiments on the data category of dresses to reduce the complexity of the experiments and the algorithms.

The experiments were conducted in *Python 3* [11], using the machine learning framework *PyTorch* [8] and several common python packages, such as: *pandas* [7], *numpy* [4], *scikit-learn* [9], *matplotlib* [3], *PIL* [6] and others.

4.1 Products to Models Translation

Most fashion online stores provide product images that are taken on white background without a person modeling the product. However, there are also countless images online, coming from social media, blogs and other platforms, of people wearing a certain product, without a corresponding product image.

The goal of this experiment was to translate a product image to an image of a person wearing that product, in order to be able to extend the search possibilities.

I have deducted several experiments, first using an unsupervised GAN, translating between the domain of all product images and the domain of all model images. This approach has not yielded the desired results, since the model images were Therefore I have decided to train the network in a supervised manner, creating a dataset of image pairs using clustering algorithms.

4.1.1 Test Environment

Data

As mentioned in Section 3.1, each scraped product has a variable amount of images of people modeling the given product. The average amount of images for a product is 4, and based on manual screening of the dataset, these images follow a certain pattern:

- full-body model front-facing
- full-body model back-facing
- zoom to part of body were product is worn
- large zoom on detail

For the used data category "dresses", there is 15.348 product images and 63.103 model images in total. Since this experiment is a pure image-to-image translation task, no attribute parsing was required.

4.1.2 Data Clustering

As mentioned in Section 3.1, each scraped product has a variable amount of images displaying people modeling the given product. The average amount of

images for a product is 4, and based on manual screening of the dataset, these images follow a certain pattern:

- full-body model front-facing
- full-body model back-facing
- zoom to part of body were product is worn
- large zoom on detail

In order to create a dataset of image pairs, each product must have exactly 1 corresponding model image. I chose the most common and basic model image - where the model is facing the camera and the full body is captured. However, there is no clear order or pattern from which to deduce the pose of the model based on the name of the image or its position the list of images. Since there are more than 60.000 model images only for category dresses, manual selection of the best image for each product would be too time consuming.

To identify the best image for each product, I used the following approach:

1. **Select Features**: Select most relevant visual features such as contours of the person in the image
2. **Image Processing**: Highlight the selected features in the image, while suppressing irrelevant features, such as color
3. **Clustering**: Cluster features and experiment with amount of clusters
4. **Select Best Cluster**: Visualize clusters and manually select the cluster with most sensible results
5. **Select Best Image**: For each product, select the image which distance to the best cluster center is the smallest

For clustering, I used the *K-Means Clustering* algorithm [2], which creates k clusters and assigns each data point to the nearest cluster center. The *scikit-learn* library offers a fast implementation of the algorithm [10].

Grayscale Clustering

Since most of the models are photographed on a white background, for the initial experiment, I have converted the images to grayscale, in order to separate the person from the background regardless of the color.

In order to reduce the dimensionality, I resized the images to 64x64 pixels, which means the clustering algorithm was fed with an array of size 63103x64x64, the first number representing the number of images.

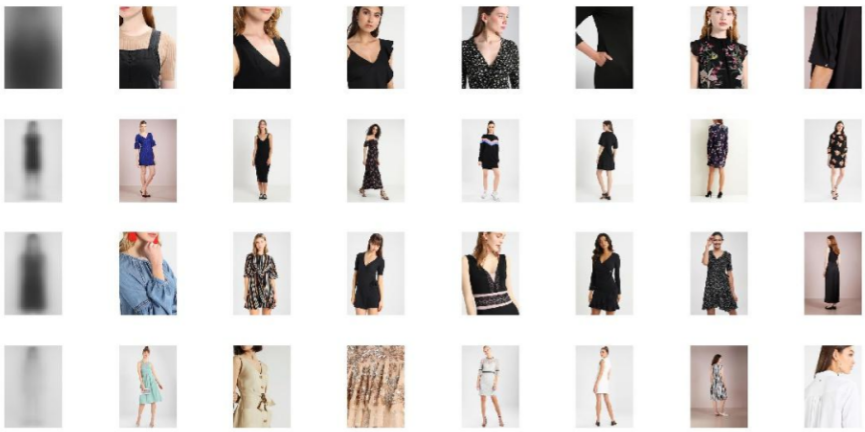

Figure 15: **Cluster centers with grayscale features.** Each row displays one cluster center (left-most image) and random images from the dataset that are assigned to the respective cluster center based on their grayscale feature vector.

Figure 15 shows the results of K-Means clustering with 4 cluster centers. The second cluster center seems to be the most suitable to find front-facing full-body images. However, as one can see from the results, the fourth cluster center tends to group all images with light-colored dresses, in all poses. Grayscale features do not fit the requirement for the clustering process to disregard color as a feature.

Edges

In order to avoid the problem of separating dark and light colors into different clusters regardless of model pose, I used the *Canny Edge Detection* algorithm on the model images, in order to only select model contours.

As part of the data collection process, all images were resized to a uniform size of 256x256, extending the shorter side with white color. However, some models are photographed on a darker background and the edge detection algorithms can detect this transition of light-grey background to white as an edge. One can observe this artifact on the second and fourth image in Figure 16.

Some clustering experiments were affected by this detection and tended to group images with darker backgrounds together, regardless of the model pose. Therefore, in all further experiments, the images have center-cropped width of 116 pixels.

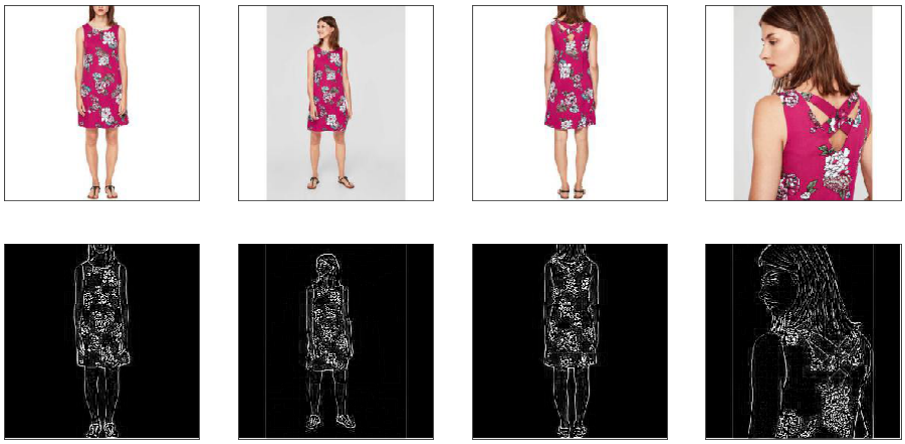

Figure 16: **Canny Edge Detection for model images.** Top row shows original data, second row shows the corresponding edges produced with Canny Edge detection algorithm.

Overall, clustering with *Canny Edge Detection* did not prove to be effective, as the edges are very thin and therefore the measured distance between two images, which are quite similar, but a little bit shifted, would be very big. The detection is also quite sensitive to patterns in the dresses, as seen in Figure 16.

Threshold Mask

To avoid the difficulties that thin edges cause when clustering, I applied a thresholding technique to the images, in order to fill the person's contour with white color and background with black. Figure 17 shows the steps applied to each image to get a binary threshold mask.

Figure 17: **Threshold Mask for model images.** Starting from left is the original image, converted to grayscale, applied Gaussian blur, binary threshold, and the image masked with binary threshold.

This feature selection has proven to be the most effective for *K-Means* algorithm with 3 cluster centers. First column of Figure 18 shows the three cluster

centers: the first groups full-body photographs, second groups zoomed images of upper-body and the last one groups detail images.

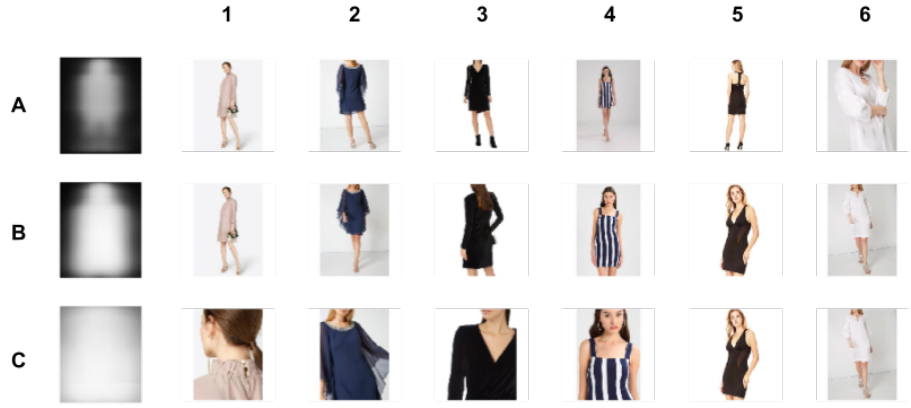

Figure 18: **Cluster centers with threshold mask.** The rows A-C show 3 cluster centers created with the *K-Means Clustering* algorithm with threshold mask features of images. Each row 1-6 shows one product and the image that is closest to the respective cluster center.

Columns 1-6 of Figure 18 each show images of one product, each row shows the image that is the closest to the respective cluster. Each product can have more photographs that are not displayed because they are not the best match for any of the cluster centers, just like one photograph can be best match for more than one cluster center. We can observe that most of the photographs are grouped accordingly to expectations.

Based on these results, I selected the one image for each product that is the closest to cluster center **A** from Figure 18. Although the results are not perfect, the network working with this data should be able to learn to ignore the outliers.

4.1.3 Supervised Training

The only network from the evaluated options that translates images in a supervised matter is Pix2Pix [18]. I have used the official PyTorch implementation of the paper [1], which can be found on github: github.com/junyanz/pytorch-CycleGAN-and-pix2pix.

5 Other

5.1 Model Images

For some of the tasks of this project also images of people modeling the products were required. However, each product, has multiple images of a model wearing it, and for the purposes of this project, I had to use clustering methods to filter out only images where the models are facing the front and photographed full-bodied.

5.1.1 Clustering

The supervised algorithms require a paired image set - in the case of generating model image from product image, it was neccessary to obtain images showing a person modelling the product. This could be obtained from the scraped websites, however each product usually has multiple model images - unordered, usually front-facing, back-facing, detail and cut. I have applied the K-Means clustering algorithm in order to separate these types of images, and for each product, find the front-facing model image.

6 Products to Models

One of the tasks of the framework is to generate a realistic image of a model wearing a product, given an image of the product. The motivation is to expand the amount of similar images found - as some products might not have a photograph without a model available at all.

I acquired the dataset for this task by downloading all model images for each product, as listed in the scraped data file. However, each product usually has multiple images with variety of model poses and detail; usually unordered and with no pattern that would indicate which image displays what pose. Therefore I have applied the K-means clustering algorithm to try to cluster these image by the model pose and for each product, select the image where the model is photographed front-facing and full-bodied.

6.1 Clustering

References

[1] Junyanz/pytorch-CycleGAN-and-pix2pix: Image-to-image translation in PyTorch (e.g., horse2zebra, edges2cats, and more), . URL https://github.com/junyanz/pytorch-CycleGAN-and-pix2pix.

[2] K-means clustering, . URL https://en.wikipedia.org/w/index.php?title=K-means_clustering&oldid=855299299. Page Version ID: 855299299.

[3] Matplotlib: Python plotting — Matplotlib 2.2.3 documentation, . URL https://matplotlib.org/.

[4] NumPy — NumPy, . URL http://www.numpy.org/.

[5] Picsbuffet, . URL https://picsbuffet.com/fotolia/#0,147,1576.

[6] Pillow — Pillow (PIL Fork) 5.3.0.dev0 documentation, . URL https://pillow.readthedocs.io/en/latest/#.

[7] Python Data Analysis Library — pandas: Python Data Analysis Library, . URL https://pandas.pydata.org/.

[8] PyTorch, . URL https://pytorch.org/.

[9] Scikit-learn: Machine learning in Python — scikit-learn 0.19.2 documentation, . URL http://scikit-learn.org/stable/.

[10] Sklearn.cluster.KMeans — scikit-learn 0.19.2 documentation, . URL http://scikit-learn.org/stable/modules/generated/sklearn.cluster.KMeans.html.

[11] Welcome to Python.org, . URL https://www.python.org/.

[12] Y. Choi, M. Choi, M. Kim, J.-W. Ha, S. Kim, and J. Choo. StarGAN: Unified Generative Adversarial Networks for Multi-Domain Image-to-Image Translation. URL http://arxiv.org/abs/1711.09020.

[13] I. Goodfellow, J. Pouget-Abadie, M. Mirza, B. Xu, D. Warde-Farley, S. Ozair, A. Courville, and Y. Bengio. Generative Adversarial Nets. In Z. Ghahramani, M. Welling, C. Cortes, N. D. Lawrence, and K. Q. Weinberger, editors, *Advances in Neural Information Processing Systems 27*, pages 2672–2680. Curran Associates, Inc. URL http://papers.nips.cc/paper/5423-generative-adversarial-nets.pdf.

[14] C. Hesse. Image-to-Image Demo - Affine Layer, . URL https://affinelayer.com/pixsrv/.

[15] C. Hesse. Image-to-Image Translation in Tensorflow - Affine Layer, . URL https://affinelayer.com/pix2pix/.

[16] X. Huang, M.-Y. Liu, S. Belongie, and J. Kautz. Multimodal Unsupervised Image-to-Image Translation. URL http://arxiv.org/abs/1804.04732.

[17] S. Ioffe and C. Szegedy. Batch Normalization: Accelerating Deep Network Training by Reducing Internal Covariate Shift. URL http://arxiv.org/abs/1502.03167.

[18] P. Isola, J.-Y. Zhu, T. Zhou, and A. A. Efros. Image-to-Image Translation with Conditional Adversarial Networks. URL http://arxiv.org/abs/1611.07004.

[19] T. Karras, T. Aila, S. Laine, and J. Lehtinen. Progressive Growing of GANs for Improved Quality, Stability, and Variation. URL http://arxiv.org/abs/1710.10196.

[20] T. Kim. DCGAN-tensorflow: A tensorflow implementation of "Deep Convolutional Generative Adversarial Networks". URL https://github.com/carpedm20/DCGAN-tensorflow.

[21] G. Lample, N. Zeghidour, N. Usunier, A. Bordes, L. DENOYER, and M. A. Ranzato. Fader Networks:Manipulating Images by Sliding Attributes. In I. Guyon, U. V. Luxburg, S. Bengio, H. Wallach, R. Fergus, S. Vishwanathan, and R. Garnett, editors, *Advances in Neural Information Processing Systems 30*, pages 5967–5976. Curran Associates, Inc. URL http://papers.nips.cc/paper/7178-fader-networksmanipulating-images-by-sliding-attributes.pdf.

[22] Y. LeCun and Y. Bengio. Convolutional Networks for Images, Speech, and Time-Series.

[23] Y. LeCun, C. Cortes, and C. Burges. MNIST handwritten digit database. URL http://yann.lecun.com/exdb/mnist/.

[24] Z. Liu, P. Luo, S. Qiu, X. Wang, and X. Tang. DeepFashion: Powering Robust Clothes Recognition and Retrieval with Rich Annotations. In *Proceedings of IEEE Conference on Computer Vision and Pattern Recognition (CVPR)*. URL http://mmlab.ie.cuhk.edu.hk/projects/DeepFashion/AttributePrediction.html.

[25] M. Mirza and S. Osindero. Conditional Generative Adversarial Nets. URL http://arxiv.org/abs/1411.1784.

[26] A. Odena, C. Olah, and J. Shlens. Conditional Image Synthesis With Auxiliary Classifier GANs. URL http://arxiv.org/abs/1610.09585.

[27] D. Pathak, P. Krahenbuhl, J. Donahue, T. Darrell, and A. A. Efros. Context Encoders: Feature Learning by Inpainting. URL http://arxiv.org/abs/1604.07379.

[28] A. Radford, L. Metz, and S. Chintala. Unsupervised Representation Learning with Deep Convolutional Generative Adversarial Networks. URL http://arxiv.org/abs/1511.06434.

[29] S. Reed, Z. Akata, X. Yan, L. Logeswaran, B. Schiele, and H. Lee. Generative Adversarial Text to Image Synthesis. URL http://arxiv.org/abs/1605.05396.

[30] rkjones4. GANGogh: Using GANs to create Art. URL https://github.com/rkjones4/GANGogh.

[31] P. D. K.-U. B. J. H. N. H. M. K. A. Sonnenberg. Akiwi - a keywording tool. URL http://www.akiwi.eu.

[32] J. T. Springenberg, A. Dosovitskiy, T. Brox, and M. Riedmiller. Striving for Simplicity: The All Convolutional Net. URL http://arxiv.org/abs/1412.6806.

[33] D. Yoo, N. Kim, S. Park, A. S. Paek, and I. S. Kweon. Pixel-Level Domain Transfer. URL http://arxiv.org/abs/1603.07442.

[34] J.-Y. Zhu, T. Park, P. Isola, and A. A. Efros. Unpaired Image-to-Image Translation using Cycle-Consistent Adversarial Networks. URL http://arxiv.org/abs/1703.10593.